



Omega-3 polyunsaturated fatty acids preserve retinal function in type 2 diabetic mice

Citation

Sapieha, P, J Chen, A Stahl, M R Seaward, T L Favazza, A M Juan, C J Hatton, J-S Joyal, N M Krah, R J Dennison, J Tang, T S Kern, J D Akula, and L E H Smith. 2012. Omega-3 polyunsaturated fatty acids preserve retinal function in type 2 diabetic mice. *Nutrition & Diabetes* 2(7): e36.

Published Version

doi:10.1038/nutd.2012.10

Permanent link

<http://nrs.harvard.edu/urn-3:HUL.InstRepos:10464949>

Terms of Use

This article was downloaded from Harvard University's DASH repository, and is made available under the terms and conditions applicable to Other Posted Material, as set forth at <http://nrs.harvard.edu/urn-3:HUL.InstRepos:dash.current.terms-of-use#LAA>

Share Your Story

The Harvard community has made this article openly available.
Please share how this access benefits you. [Submit a story](#).

[Accessibility](#)

ORIGINAL ARTICLE

Omega-3 polyunsaturated fatty acids preserve retinal function in type 2 diabetic mice

P Sapieha^{1,2,5}, J Chen^{1,5}, A Stahl^{1,3}, MR Seaward¹, TL Favazza¹, AM Juan¹, CJ Hatton¹, J-S Joyal¹, NM Krah¹, RJ Dennison¹, J Tang⁴, TS Kern⁴, JD Akula¹ and LEH Smith¹

OBJECTIVE: Diabetic retinopathy (DR) is associated with hyperglycemia-driven microvascular pathology and neuronal compromise in the retina. However, DR is also linked to dyslipidemia. As omega-3 (ω -3) polyunsaturated fatty acids (PUFAs) are protective in proliferative retinopathy, we investigated the capacity of ω -3PUFAs to preserve retinal function in a mouse model of type 2 diabetes mellitus (T2DM).

DESIGN: Male leptin-receptor-deficient (*db/db*) mice were maintained for 22 weeks (4 weeks–26 weeks of life) on calorically and compositionally matched diets, except for 2% enrichment in either ω -3 or ω -6PUFAs. Visual function was assessed at 9, 14 and 26 weeks by electroretinography. Retinal capillary and neuronal integrity, as well as glucose challenge responses, were assessed on each diet.

RESULTS: The ω -3PUFA diet significantly preserved retinal function in the mouse model of T2DM to levels similar to those observed in nondiabetic control mice on normal chow. Conversely, retinal function gradually deteriorated in *db/db* mice on a ω -6PUFA-rich diet. There was also an enhanced ability of ω -3PUFA-fed mice to respond to glucose challenge. The protection of visual function appeared to be independent of cytoprotective or anti-inflammatory effects of ω -3PUFAs.

CONCLUSION: This study identifies beneficial effects of dietary ω -3PUFAs on visual function in T2DM. The data are consistent with dyslipidemia negatively impacting retinal function. As ω -3PUFA lipid dietary interventions are readily available, safe and inexpensive, increasing ω -3PUFA intake in diabetic patients may slow the progression of vision loss in T2DM.

Nutrition and Diabetes (2012) 2, e36; doi:10.1038/nutd.2012.10; published online 23 July 2012

Keywords: diabetic retinopathy; omega-3 PUFAs; electroretinography

INTRODUCTION

Diabetic retinopathy (DR) is a major complication of diabetes and the most frequent cause of blindness in ages 30–60 years.¹ The number of patients with diabetes worldwide is projected to be 366 million by 2030,² with type 2 diabetes mellitus (T2DM) accounting for the greatest increase in new cases. It is estimated that over 80% of patients afflicted with T2DM will develop a form of DR within 20 years of diagnosis.³ Clinically, DR is first seen as a progressive loss of retinal vasculature (nonproliferative DR) characterized by microaneurysms, pericyte loss and basement membrane thickening.⁴ Importantly, often preceding vascular changes, retinal neurons, including retinal ganglion cells (RGCs), are damaged.^{5–7} Nonproliferative DR is also associated with increased inflammation, increased vascular permeability and leukostasis. In response to retinal hypoxia resulting from the vessel loss in nonproliferative DR,⁸ there is a second phase consisting of pathological vasoproliferation (proliferative DR), which can cause tractional retinal detachment leading to blindness.

Besides hyperglycemia, dysregulation of lipid metabolism is associated with DR. Modulating a patient's lipid profile^{9–11} can improve DR. Lipids have important regulatory roles beyond energy storage and membrane structure. Importantly, intake of

essential omega-3 (ω -3) long-chain polyunsaturated fatty acids (PUFAs) directly influences lipid signaling and has therapeutic potential in metabolic and inflammatory conditions.^{12,13} As mammals are not readily capable of synthesizing ω -3 and ω -6PUFAs, the content of these PUFAs in tissue is almost solely defined via dietary intake.

In a mouse model of oxygen-induced retinopathy with characteristics of proliferative DR, we have previously demonstrated that a diet enriched in ω -3PUFAs (similar to human Japanese diets) effectively reduces pathological retinal neovascularization when compared with an ω -6PUFA-rich diet (mimicking human American diets).^{14–16}

These findings are consistent with the human Age-Related Eye Disease Study reports, which found that total dietary intake of ω -3PUFAs is inversely associated with the risk of neovascular age-related macular degeneration.¹⁷ Moreover, a lower incidence of T2DM has been reported in individuals whose diets are rich in ω -3PUFAs.¹⁸

Although tight glycemic control retards retinopathy, compliance is difficult. A safe nutritional intervention to help prevent DR would answer a clinically unmet need. Here we present the first evidence that dietary ω -3PUFA supplementation reduces hyperglycemia, improves glucose tolerance and directly preserves

¹Department of Ophthalmology, Harvard Medical School, Children's Hospital Boston, Boston, MA, USA; ²Department of Ophthalmology, Maisonneuve-Rosemont Hospital Research Centre, University of Montreal, Montreal, Quebec, Canada; ³Department of Ophthalmology, University Eye Hospital Freiburg, Freiburg, Germany and ⁴Department of Medicine, Case Western Reserve University and Louis Stokes Veterans Hospital, Cleveland, OH, USA. Correspondence: Professor LEH Smith, Department of Ophthalmology, Harvard Medical School, Children's Hospital Boston, 300 Longwood Avenue, Boston, MA 02115, USA.
E-mail: lois.smith@childrens.harvard.edu

⁵These authors contributed equally to this work.

Received 15 March 2012; revised 25 May 2012; accepted 14 June 2012

retinal function before any detectable neuronal or vascular loss in a mouse model of type 2 diabetes (*db/db*).

MATERIALS AND METHODS

Animals

All studies adhered to the Association for Research in Vision and Ophthalmology Statement for the Use of Animals in Ophthalmic and Vision Research, and were approved by Children's Hospital Boston Animal Care and Use Committee. Institutional Animal Care and Use Committee (IAACUC) protocol number 10-08-1770R. Male *db/db* mice and nondiabetic heterozygous littermate controls (BKS.Cg-Dock7^{m+/+} Lepr^{db/J}, stock number 000642) we from The Jackson Laboratories (Bar Harbor, ME, USA).

Omega-3, ω-6PUFA diets and control chow

Mice were fed from 4 weeks to 26 weeks with defined rodent diets.^{14–16} These calorically matched rodent diets contained either 2% ω-3PUFAs (DHA and EPA) for the treatment group or 2% ω-6PUFAs (arachidonic acid) for the control group. Dietary PUFAs were produced by DSM Nutritional Products (Parsippany, NJ, USA) under the trade name ROPUFA. The arachidonic acid and DHA supplements, under the trade names ARASCO and DHASCO, respectively, were obtained from Martek Biosciences Corp. (Columbia, MD, USA). Standard rodent chow ('normal feed') from Purina (Framingham, MA, USA) was used as a control diet in *db/+* control mice for all retinal electrophysiology experiments.

Blood glucose measurements and glucose tolerance test

Body weight and baseline fasting blood glucose levels (Accu-Chek, Roche, Indianapolis, IN, USA) of the mice were recorded. Glucose tolerance tests (age 7 weeks) consisted of blood glucose measurement, then injection of 1 ml 10% D-glucose intraperitoneally, followed by blood glucose measurements at 30, 60 and 240 min.

Electroretinography

Retinal function was assessed¹⁹ at 9, 14 and 26 weeks by full-field electroretinography (ERG) in *db/db* mice fed ω-3- or ω-6PUFA chows, and in heterozygous mice on normal chow. The stimuli were 'green' light-emitting diode flashes of doubling intensity from ~0.0005 to ~2.05 cd s m⁻² and then 'white' xenon-arc flashes—half as efficient (per cd s m⁻²) at eliciting a b-wave¹⁹—from ~8.2 to ~1.050 cd s m⁻², all presented to the dark-adapted, cycloplegic eye. The response to a 1.024 cd s m⁻² green light flickering at 8 Hz in the presence of an amber background that suppressed the saturating rod photoresponse by >90% was recorded.

The saturating photoresponse was characterized from the ERG by optimization of the free parameters of the Hood and Birch²⁰ formulation of the Lamb and Pugh²¹ model of the activation of phototransduction:

$$P_3(i, t) = Rm_{P3} \cdot \left(1 - \exp\left(-1/2 \cdot i \cdot S \cdot (t - t_d)^2\right) \right) \text{ for } t_d < t < 15 \text{ ms.} \quad (1)$$

In this model, *i* is the intensity of the flash (cd s m⁻²), *t* is elapsed time (s), *Rm_{P3}* (μV) is proportional to the magnitude of the dark current, *S* (cd⁻¹ s⁻³ m²) summarizes the kinetics of phototransduction and *t_d* is a brief delay (s).

The postreceptor response, *P₂*, mostly from bipolar cells,^{22,23} was obtained by digitally subtracting *P₃* (equation (1)) from the intact ERG. The response versus intensity relationship of *P₂* was fit to the Naka-Rushton equation,

$$\frac{P_2(i)}{Rm_{P2}} = \frac{i}{i + k_{P2}}, \quad (2)$$

wherein *P₂(i)* is the amplitude (μV) of the response to a stimulus of *i* intensity, *Rm_{P2}* (μV) is the saturating bipolar response and *k_{P2}* is the flash intensity that elicits a half-maximum *P₂*; *k_{P2}*⁻¹ and *S* are suprathreshold measures of sensitivity. However, *P₂* increases in linear proportion to stimulus intensity over a narrow range of dim flash intensities,²³ and thus the sensitivity of *P₂* at threshold was defined in this range²⁴ by scaling the amplitude of each *P₂* by the intensity used to elicit it and fitting

$$\frac{Sf(i)}{Sm} = \frac{i^{-1}}{i^{-1} + \Phi_{1/2}^{-1}} \quad (3)$$

to the resulting sensitivities. *Sf(i)* is the fractional sensitivity (μV cd⁻¹ s⁻¹ m²) of the *P₂* response to a flash of *i* intensity, *Sm* is the sensitivity of the retina at threshold and *Φ_{1/2}* is the stimulus intensity at which sensitivity has fallen by half.

The oscillatory potentials (OPs) characterize activity in retinal cells distinct from those that generate *P₃* and *P₂*. The OPs were analyzed in the frequency domain following discrete Fourier transform of the first 128 ms of *P₂*.²⁵ The saturating energy in the OPs, *Em* (∞ J), was derived similarly to *Rm_{P2}* from the response versus intensity relationship of OP energy. *Em* is related to the square of OP amplitude,²⁵ and thus its root (*Em*^{1/2}) was used in all analyses.

To evaluate a cone-mediated response, the trough-to-peak amplitude of the light-adapted, 8 Hz flicker response (*R8*) was measured.

Isolation of retinal vasculature

Enucleated eyes from 26-week-old *db/db* mice were fixed in formalin. Retinal vasculature was isolated by trypsin digest,^{26,27} then dried on microscope slides and stained with hematoxylin–periodic acid Schiff. Acellular capillaries were counted (masked)²⁸ and expressed per mm² of the retina.

Retinal flatmount and RGC imaging

Ganglion cells were quantified in both central and peripheral regions of the retina in a masked fashion in 26-week-old *db/db* mouse retinas fixed in 4% paraformaldehyde, stained with β-III tubulin primary antibody (C terminus, TP1691, ECM Biosciences, Versailles, KY, USA), and then whole-mounted with the photoreceptor side down and embedded in SlowFade Antifade reagent (Invitrogen, Grand Island, NY, USA). Flatmounts were visualized and recorded with ×63 objectives on a Leica TCS SP2 Confocal microscope and Leica Confocal Software (Leica Microsystems, Buffalo Grove, IL, USA).

RNA isolation and reverse-transcription quantitative PCR

Retinas were isolated, treated with DNase I (Qiagen, Valencia, CA, USA), and then the RNA was isolated and converted into cDNA with reverse transcriptase (Invitrogen). PCR primers targeting tumor necrosis factor-α, interleukin (IL)-1β, IL-6, IL-10, intercellular adhesion molecule-1, claudin-5, plasmalemma vesicle-associated protein, β-III tubulin and control cyclophilin A were designed with Primer Bank and NCBI Primer Blast software. Quantitative analysis of gene expression was quantified with an ABI Prism 7700 and SYBRGreen Master Mix kit (Applied Biosystems, Foster City, CA, USA), and expressed relative to cyclophilin A.

Enzyme-linked immunosorbent assay measurements of inflammatory profiles

Serum was collected from mice at 26 weeks of age and analyzed for the presence of inflammatory proteins using the Multiplex-ELISA (5P30 DK 36836 Specialized Assay Core) at the Joslin Diabetes Center (Boston, MA, USA).

Statistics

ERG parameters were expressed as log values so that changes of fixed proportion became linear, and were normalized to the values obtained at each age in the heterozygous mice with normal chow so that confounding effects of the natural aging process were eliminated. Differences in ERG parameters were detected by analysis of variance followed by Tukey's honestly significant difference test. Statistical testing of anatomic and molecular biological results was limited to ω-3 and ω-6PUFA mice, and performed by two-sample *t*-test, unless otherwise indicated.

RESULTS

Dietary intake of ω-3PUFAs preserves visual function in type 2 diabetes

The development of DR is associated with progressive loss of retinal function.^{29–31} Given the potent neuroprotective effects of ω-3PUFAs³² and their propensity to be incorporated into the retina,¹⁴ we sought to determine whether dietary supplementation with these lipids could delay the onset or decrease the severity of retinal neuronal dysfunction in a mouse model of T2DM.

Male leptin-receptor deficient (*db/db*) mice were maintained for 22 weeks (from 4 weeks to 26 weeks of life) on calorically and

compositionally matched diets, except for 2% enrichment in either ω -3 or ω -6PUFAs. These rigorously defined diets are identical, except for fatty acids: 1% docosahexaenoic acid and 1% eicosapentaenoic acid for ω -3PUFAs or 2% arachidonic acid for ω -6PUFAs. Undefined and variable 'standard rodent chow' varies in its composition from batch to batch, depending on which oils happen to be available to the manufacturer at the time of feed production. For this reason, standard chow was only given to wild-type control mice as a reference.

Nondiabetic heterozygote controls were maintained on normal chow to assess baseline retinal function in healthy individuals. We performed ERGs on *db/db* and control mice throughout the progression of disease at 9, 14 and 26 weeks, and found that, in contrast to ω -6PUFAs, ω -3PUFAs significantly preserved retinal function to levels akin to wild-type control mice receiving standard chow (Figure 1a–d). With ω -6PUFAs, we observed a protracted loss in retinal function by 26 weeks of life compared with both ω -3PUFA-fed mice and age-matched control heterozygotes on standard chow (gray line; Figure 1b–d). As shown in

Figure 1a, photoreceptor (*a*-wave) and postreceptor responses (*b*-wave, OPs) were markedly attenuated. Saturating ERG response amplitudes (Figure 1b) in the *db/db* mice (whether ω -3- or ω -6PUFA-enriched) trended lower-than-normal at every test age for the three mixed rod- and cone-mediated wavelets studied, P_3 (Rm_{P_3}), P_2 (Rm_{P_2}) and the OPs ($Em^{1/2}$). Indeed, age \times group \times wavelet ERG responses in the *db/db* mice were diminished ($P < 0.0001$); however, *post-hoc* testing detected no significant difference between the ω -3PUFA *db/db* mice and the heterozygous controls, whereas ω -6PUFA *db/db* mice differed significantly from both. *Post-hoc* testing also revealed that P_2 was more attenuated than P_3 , consistent with synaptic compromise at the outer plexiform layer. The effects of age ($P = 0.009$) and age \times group ($P = 0.002$) indicated that the magnitude of the functional deficit increased at 26 weeks only in the ω -6PUFA *db/db* mice. The amplitude of the cone-isolated response to 8 Hz flicker ($R8$, Figure 1c) was also attenuated in the *db/db* mice ($P < 0.0001$). Again, effects of age ($P = 0.009$) and age \times group ($P = 0.002$) indicated that the deficit increased with age most severely in the

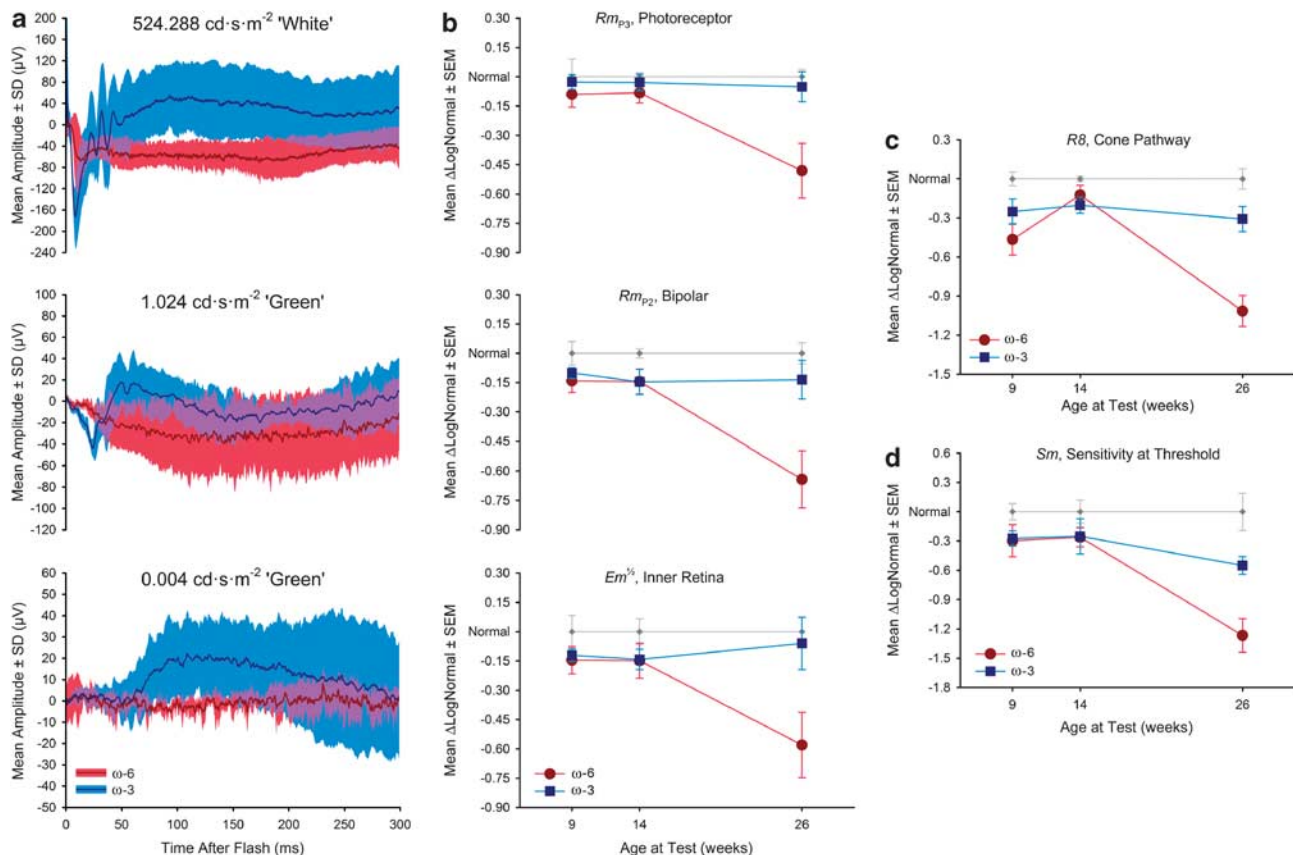


Figure 1. Omega-3 PUFA preserves retinal function in *db/db* mice. ERG assessment of *db/db* mice at 9, 14 and 26 weeks of age indicated that ω -3PUFAs preserve retinal function. (a) Selected from a dark-adapted ERG intensity series spanning a 2^{30} range of stimuli, averaged responses (lines) and one s.d. (fills) of 26-week-old mice maintained on ω -6- and ω -3PUFA-rich diets are shown; both increments are 2^8 after correcting for the retina's 50% lower sensitivity to the 'white' stimulus. The dim flash (bottom) evoked a marked *b*-wave in the ω -3PUFA-fed mice, but no detectable response in the ω -6PUFA-fed mice. The moderate flash (middle) evoked a pronounced *a*-wave in both the ω -3- and ω -6PUFA-fed mice, but did not elicit a detectable post-receptor response (*b*-wave or OPs) in the ERG of the ω -6PUFA-fed mice. The bright flash (top) evoked a saturating *a*-wave in both the ω -3- and the ω -6PUFA-fed mice. In the former, the *a*-wave was large, the OPs were pronounced and the *b*-wave rose well above baseline; in the latter, the *a*-wave was smaller, and both the *b*-wave and the OPs were strikingly enervated. (b) Mean values of ERG parameters describing the saturating amplitude of responses originating in photoreceptors, (Rm_{P_3} , top), bipolar cells (Rm_{P_2} , middle) and other postreceptor neurons ($Em^{1/2}$, bottom) are plotted for the ω -3 and ω -6 *db/db* mice after normalizing by the values in age-matched heterozygotes on normal chow (grayed data). These parameters were significantly attenuated in ω -6PUFA-fed, 26-week-old *db/db* mice. (c) The amplitude of the response to 8 Hz flicker isolated to the cone pathway by a rod-suppressing adapting background ($R8$) is plotted as in b. $R8$ was somewhat reduced in *db/db* mice fed ω -3PUFAs-rich diets, but did not degenerate; *db/db* mice fed ω -6PUFA-rich diets showed a severe decline (~ 1 log unit) in cone-pathway function at age 26 weeks. (d) Retinal sensitivity at threshold (Sm), derived from P_2 , is plotted (again as in b). Sm was somewhat low in all *db/db* mice, but was preserved by ω -3PUFAs. In contrast, ω -6-fed *db/db* mice suffered a profound loss of sensitivity (> 1.2 log units).

ω -6PUFA-fed *db/db* mice. The deficit was larger for this cone-isolated response than for the mixed rod/cone responses: ~ 1 log unit versus ~ 0.6 log units. In addition, *R8* in both the ω -3 and ω -6 *db/db* mice differed significantly from the heterozygous controls.

Suprathreshold sensitivity parameters (S , k_{p2}^{-1}) did not differ between the ω -3 and ω -6PUFA *db/db* mice (data not shown). However, retinal sensitivity at threshold (S_m , Figure 1d), which depends on the function of both the photoreceptors and bipolar cells, was low in the *db/db* mice ($P < 0.0001$), especially in those maintained on the ω -6PUFA diet. Again, *post-hoc* testing, and effects of age ($P = 0.001$) and age \times group ($P = 0.01$) revealed that the loss in sensitivity in the ω -3PUFA-fed mice was significantly less than in the ω -6PUFA-fed mice.

These data indicate that ω -3PUFAs effectively preserve retinal function in T2DM. The average weight of ω -3- and ω -6PUFA-fed mice did not vary significantly in *db/db* mice or in control heterozygotes (Supplementary Figure 1), although the *db/db* and heterozygotes did differ from one another.

Omega-3-Rich diets enhance glucose homeostasis in *db/db* mice
Epidemiological studies show a lower incidence of T2DM in individuals who consume higher levels of ω -3PUFAs,¹⁸ and ω -3PUFAs may enhance tolerance to systemic spikes in glucose.^{33,34} To evaluate the influence of ω -3PUFA-rich diets on glucose homeostasis, we first measured fasting baseline glycemia in *db/db* and heterozygous *db/+* controls. Omega-3PUFA-fed mice persistently demonstrated lower blood glucose levels at 10 ($P = 0.0087$), 13 ($P = 0.0203$) and 16 ($P = 0.0205$) weeks; (Figure 2a).

Glucose tolerance tests on mice of 7 weeks of age showed improved glucose excretion from serum in ω -3-fed *db/db* mice (at 30 min) when compared with ω -6PUFA-fed mice ($P = 0.0379$) (Figure 2b). A similar benefit was noted in heterozygous control mice, with ω -3PUFA-rich diets significantly improving glucose tolerance compared with normal chow ($P = 0.0025$; Figure 2c). Thus, ω -3PUFA-fed T2DM mice responded more normally to

spikes in glucose, suggesting that diets rich in ω -3PUFAs confer a protective systemic effect against the early manifestation of T2DM.

The protective effects of ω -3PUFA-rich diets on retinal function are independent of gross retinal cytoprotection

A primary manifestation of intermediate stage DR is the degeneration of microvascular capillaries. Similar densities of acellular capillaries were found in *db/db* mice on either diet ($P = 0.1973$; Figures 3a–c), suggesting that the observed preservation in ERGs is independent of any ω -3PUFA-mediated preservation of retinal vasculature integrity.

During progression of DR, there is specific loss of RGCs^{5,6} in humans^{35,36} and animal models.^{6,37,38} It is speculated that loss of RGCs may precede the vascular manifestation of the disease. We assessed if the heightened retinal function observed in ω -3-fed *db/db* mice was secondary to RGC neuroprotection. Equal numbers of RGCs are present in ω -3- and ω -6PUFA-fed mice (Figures 3d and e) in both central ($P = 0.5538$) and peripheral ($P = 0.8599$) zones of the retina (Figure 3f). In line, the expression of retinal β III-tubulin mRNA remains constant, confirming that RGC numbers are equivalent in mice receiving either diet ($P = 0.6698$; Figure 3g). Similarly, we did not detect any appreciable morphological differences in photoreceptors, or in the thickness of the outer nuclear layer (Figures 3h–j). Consistent with these observations, the mRNA levels of cone opsin (Figure 3k) or rhodopsin (Figure 3l)³⁹ did not significantly vary between the feed groups, suggesting similar photoreceptor numbers between the feed groups. Taken together, these data suggest that the benefit in retinal function observed in ω -3PUFA-fed *db/db* mice precedes detectable anatomic changes in retinal vasculature and RGC integrity, and may be independent of the vasoprotective effects of ω -3PUFAs.

The protective effects of ω -3PUFA-rich diets on retinal function are independent of inflammatory modulation

Given the anti-inflammatory effects of ω -3PUFAs⁴⁰ and the role of inflammation in DR, we determined the inflammatory status of the

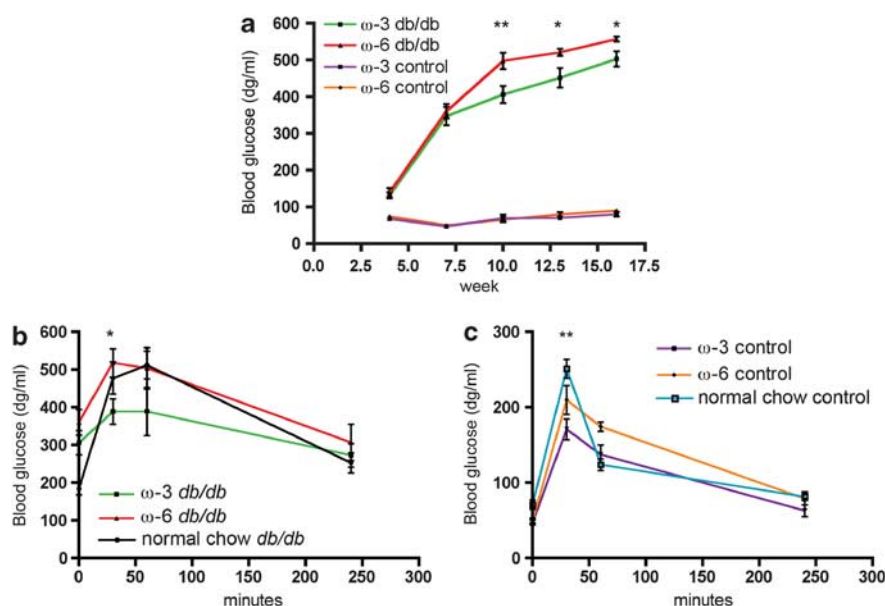


Figure 2. Dietary ω -3PUFAs improve glucose tolerance in *db/db* mice. (a) Fasting baseline blood glucose levels measured in ω -3 and ω -6PUFA-fed *db/db* mice showed significantly lower blood glucose levels at 10, 13 and 16 weeks in ω -3PUFA-fed *db/db* mice ($*P < 0.05$; $**P < 0.01$; $n = 14$ per group). Baseline glycemia did not vary between the two feed groups in control nondiabetic heterozygotes *db/+* mice. (b) Glucose tolerance tests reveal ω -3PUFA-fed *db/db* mice to be significantly protected against glycemic spikes 30 min after glucose injection ($*P < 0.05$; $n = 5$ per group). (c) A similar protective pattern by ω -3PUFA feed was noted in nondiabetic heterozygote control mice. ($*P < 0.05$, $**P < 0.01$; $n = 5$ per group).

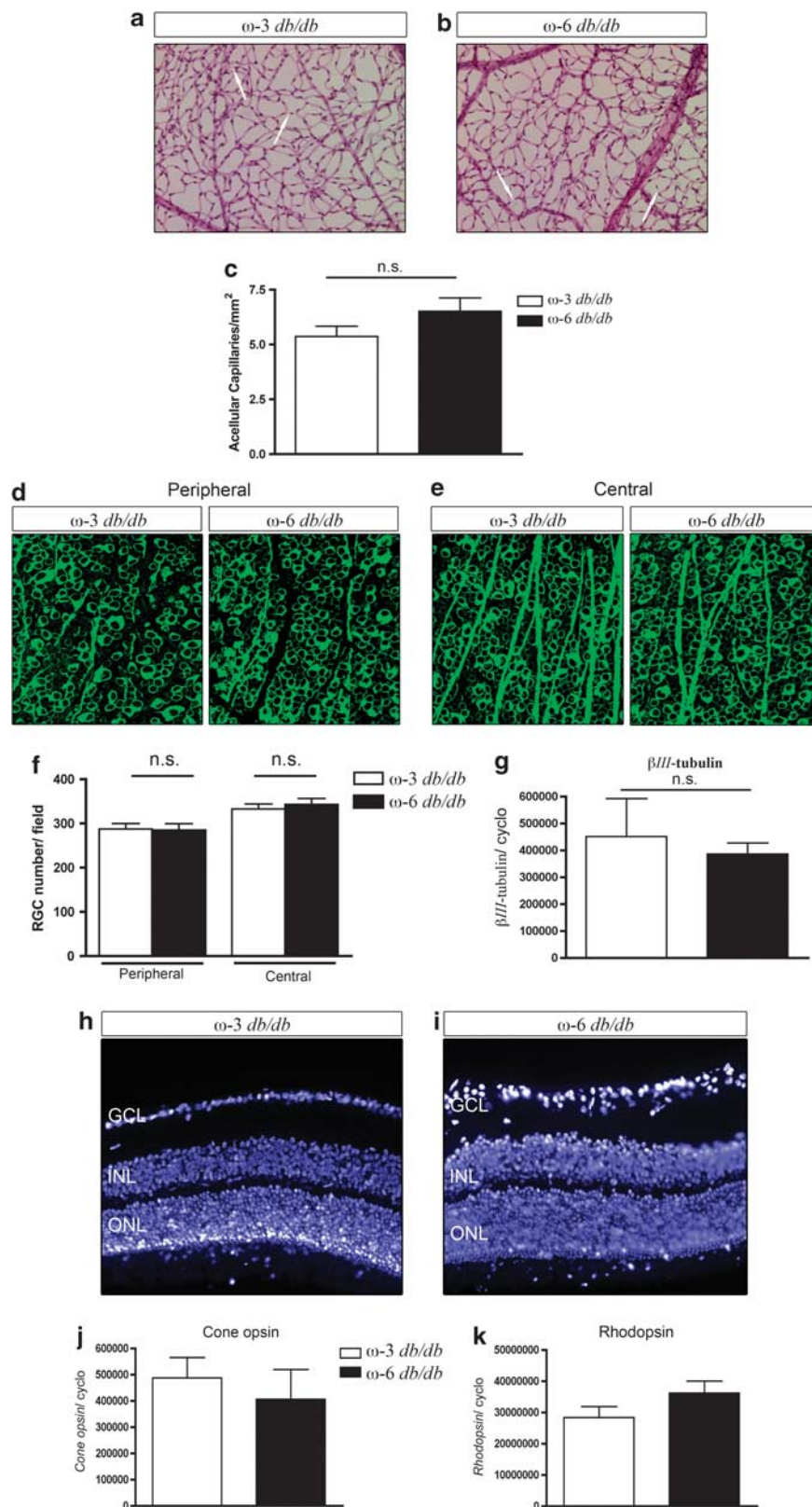


Figure 3. Lack of change in acellular capillary, retinal ganglion cell and photoreceptor densities in *db/db* mice on ω -3 or ω -6PUFA feeds. Representative images of retinal capillaries from ω -3- (**a**) or ω -6PUFA-fed (**b**) *db/db* mice at 26 weeks of age reveal no statistically significant change in the number of acellular capillaries (white arrows) as quantified in (**c**). Representative images of β -III tubulin-stained RGCs from the peripheral (**d**) and central regions (**e**) of retinas from ω -3- and ω -6PUFA-fed *db/db* mice at 26 weeks reveal no statistically significant change in total numbers between feed groups (**f**). (**g**) Real-time qPCR quantification of β -III tubulin from whole retinas of 26-week-old *db/db* mice (normalized to millions of copies of Cyclophilin A (cyclo) mRNA) confirm comparable numbers of RGCs in both feeds; $n = 7$ retinas for ω -3PUFA and $n = 5$ for ω -6PUFA group. Photoreceptor densities were unaffected by feeds. 4',6-diamidino-2-phenylindole (DAPI)-stained retinas from ω -3- (**h**) and ω -6-fed (**i**) *db/db* mice at 26 weeks of age revealed that photoreceptor densities were unaffected. Real-time qPCR quantification of cone opsin (**j**) and rhodopsin (**k**) mRNA.

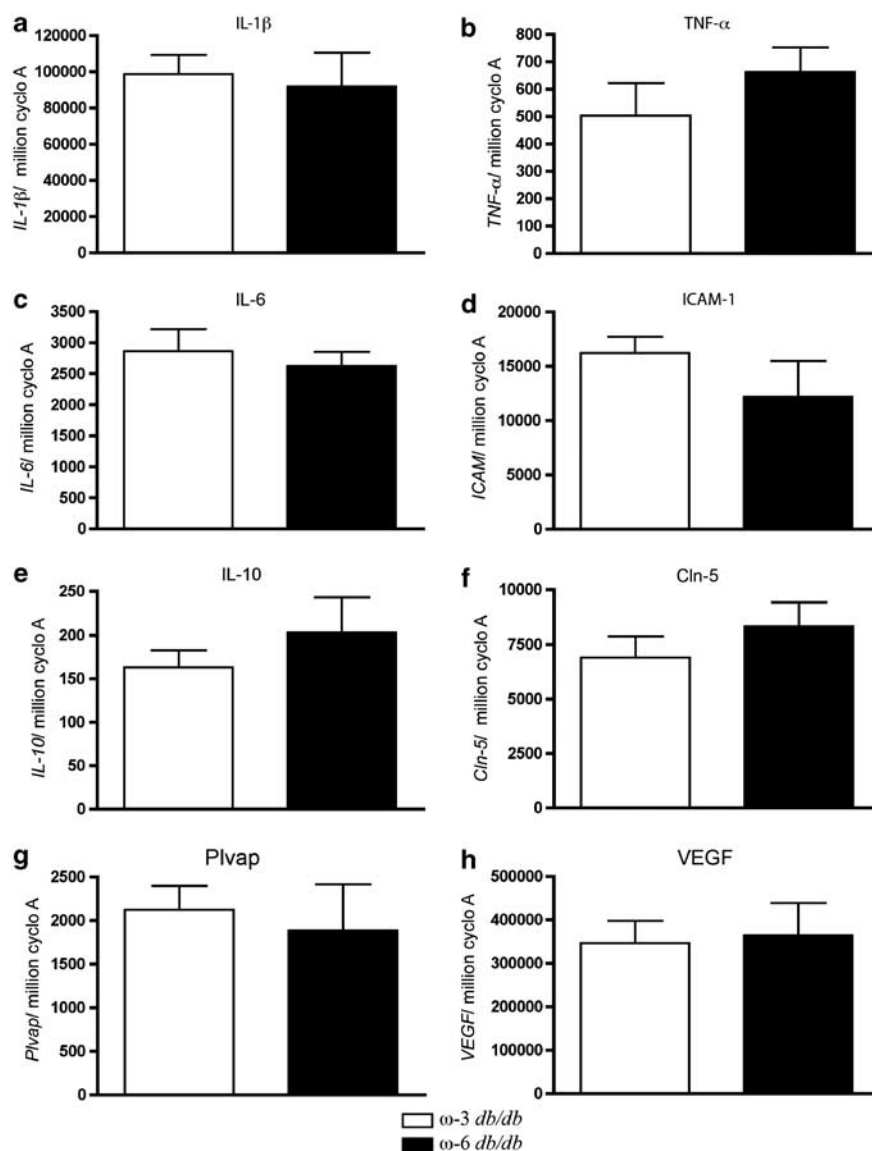


Figure 4. Inflammation and permeability markers in *db/db* retinas do not vary with ω -3 or ω -6PUFA feeds. Real-time qPCR for inflammatory cytokines at 26 weeks ((a) IL-1 β , (b) tumor necrosis factor (TNF)- α , (c) IL-6, (d) intercellular adhesion molecule-1 and (e) the anti-inflammatory cytokine IL-10) reveal no change in inflammatory profiles between feeds at this stage of the disease. Similarly, tight-junction protein claudin-5 (Cln-5) (f), cell-permeability markers plasmalemma vesicle-associated protein (Plvap) (g), and permeability and angiogenic factor vascular endothelial growth factor (VEGF) (h) do not vary with feed. All genes are normalized to copies of Cyclophilin A (cyclo A) mRNA; $n=5$ mice per group.

retina in ω -3- and ω -6PUFA-fed *db/db* mice. At 26 weeks, corresponding to the time point of maximal measured discrepancy in ERG signal between ω -3- and ω -6PUFA-fed *db/db* mice, (Figure 1) all tested inflammatory cytokines, including IL-1 β ($P=0.7484$; Figure 4a), IL-6 ($P=0.6163$; Figure 4c), tumor necrosis factor- α ($P=0.3456$; Figure 4b), intercellular adhesion molecule-1 ($P=0.2976$; Figure 4d) and the anti-inflammatory IL-10 ($P=0.4296$; Figure 4e), showed similar retinal mRNA expression levels in animals receiving either ω -3- or ω -6PUFA-rich diets.

We next assessed the expression of key constituents of vascular barrier function. As with the profiles of inflammatory mediators, retinal mRNA levels of the tight-junction protein claudin-5 ($P=0.3501$; Figure 4f) and plasmalemma vesicle-associated protein, an indicator of vessel permeability^{41,42} ($P=0.7220$; Figure 4g) did not vary with feeds and neither did vascular endothelial growth factor ($P=0.8449$; Figure 4h). Similarly, protein levels of the key inflammatory mediators did not vary with feed in

the serum of ω -3- and ω -6-fed mice: IL-1 β ($P=0.9046$; Figure 5a), tumor necrosis factor- α ($P=0.7609$; Figure 5b), IL-6 ($P=0.9362$; Figure 5c) and IL-10 ($P=0.8857$; Figure 5d). Moreover, systemic levels of VEGF remained unaffected by feed ($P=0.9576$; Figure 5e), as did the levels of insulin ($P=0.2020$; Figure 5f). Taken together, our data suggest that the protective effects of ω -3PUFAs on retinal function in T2DM occur independently of inflammation, cell survival or barrier function, suggesting that ω -3-rich diets robustly protect neuronal function via a mechanism independent of or preceding macrocellular changes.

DISCUSSION

The clinical diagnosis of DR presently relies entirely on the detection of vascular lesions such as capillary degeneration, retinal edema and hemorrhages (in early stages), or neovascular

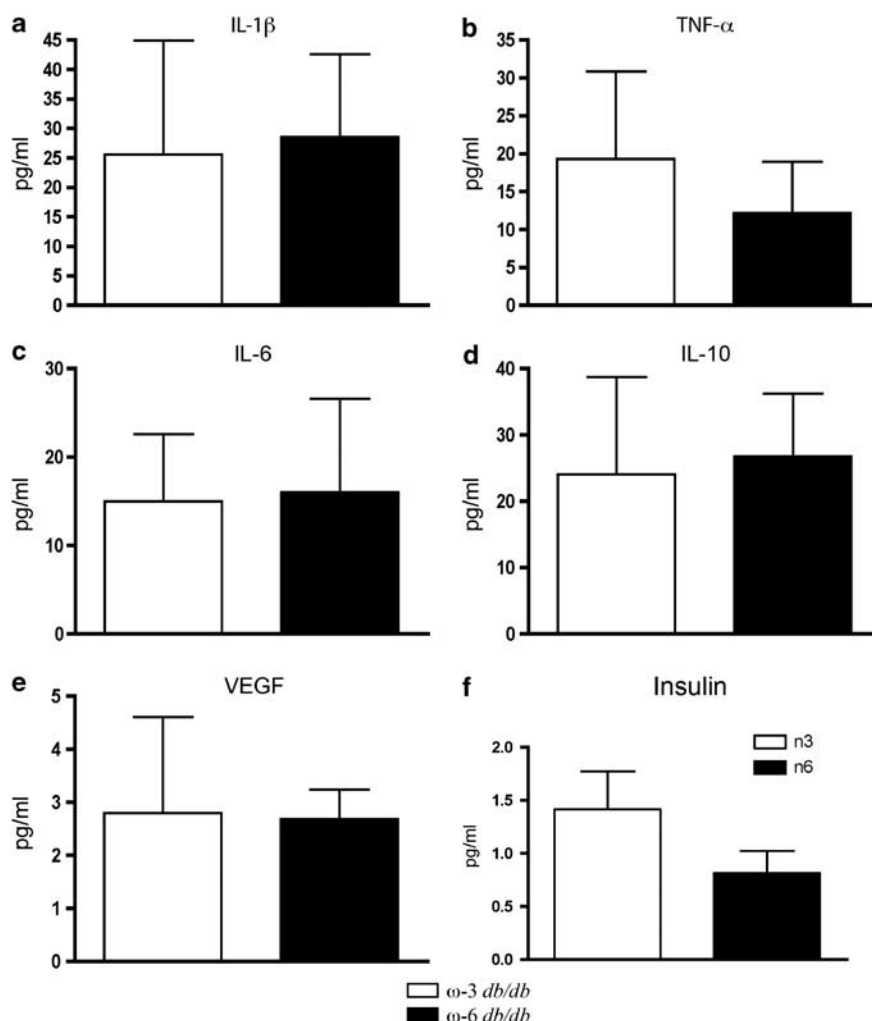


Figure 5. Systemic markers of inflammation in serum of *db/db* mice do not vary with ω -3 or ω -6PUFA feeds. ELISA measurements performed on serum at 26 weeks; ((a) IL-1 β , (b) tumor necrosis factor (TNF)- α , (c) IL-6 and (d) the anti-inflammatory cytokine IL-10) reveal no change in inflammatory profiles between feeds at this stage of the disease. Similarly, vascular endothelial growth factor (VEGF) levels (e) and insulin (f) do not vary with feed; $n = 5$ mice per group.

proliferation (in later stages). This has led to the general presumption that the disease is exclusively microvascular in nature and that effective treatments would have to either directly counter stressors to the endothelium or alleviate the burden of pro-angiogenic factors present in the vitreous. On the other hand, T2DM is also characterized by a general metabolic dysregulation and systemic dyslipidemia.⁴³ By directly modulating dietary lipid consumption to favor ω -3PUFA intake, we efficiently stalled the deterioration of retinal visual function associated with DR before any vasoprotective effects, and independent of the anti-inflammatory properties of these lipids. This suggests that ω -3PUFAs have the capacity to protect cellular function in DR and thus delay the early events of diabetes-induced neuronal dysfunction in the retina. With a 2% change in fatty acid content (ω -3 vs ω -6), there is a two-fold increase in retinal ω -3 levels,¹⁴ and this is also reflected in erythrocyte composition. It is however important to note that the diabetic-like phenotype observed in *db/db* mice results secondarily to dyslipidemia and obesity, and therefore specific changes in lipid metabolism may differ from that observed in human type 2 diabetes. Hence, it is conceivable that lipid supplementation protocols could have beneficial effects in *db/db* mice that differ from human diabetic patients.

Although the mechanisms assuring the functional protection of the neural retina by ω -3PUFAs presently remain elusive, it is important to note that the observed benefits were accompanied by enhanced glucose tolerance in ω -3PUFA-fed mice. Neurons require a steady supply of glucose and thus cannot rely on glycolytic bursts nor depend on episodic insulin-driven glucose uptake.⁴⁴ Consequently, neuronal glucose uptake is highly dependent on the insulin-unresponsive GLUT-1,⁴⁵ and thus the extracellular concentrations of glucose. Persistent hyperglycemia in diabetes can result in sustained levels of neuronal glucose up to fourfold in healthy individuals and lead to glucose neurotoxicity.⁴⁶ It is therefore tempting to speculate that the lower systemic glycemia and significantly improved ability to respond to glucose challenge in ω -3PUFA-fed animals may contribute, in part, to the protective effects of ω -3PUFAs on neuronal function. It is noteworthy that there is a loss of weight in ω -6PUFA-fed mice that commences after 12 weeks of life (Supplementary Figure 1), suggesting that animals on these diets thrive less than those on ω -3PUFA-rich diets.

Although we observed a beneficial effect of ω -3PUFA-rich diets on the preservation of retinal function in T2DM, our study has limitations. For example, retinal samples were collected and analyzed subsequent to the final ERG recordings at 26 weeks

of age. It is therefore conceivable that a change in inflammatory profiles occurred at an earlier time point, but normalized by 26 weeks of age. Conversely, it is also possible that gross changes in retinal structure, such as capillary dropout and RGC loss, would be detected at later time points than those sampled. However, we carried out these analyses at a time corresponding to the greatest discrepancy in retinal function between our treatment groups. Although the functional protection afforded by the ω -3-rich diets did not show detectable cellular preservation, our study was not designed to account for discrepancies in cell-cell interaction nor for differences in retinal signaling.

Given that the current treatment modalities to counter DR are costly, invasive and unproven for the long term, nutritional interventions have the potential to result in a significant improvement over existing approaches in that the proposed ω -3PUFA lipid-based strategies are readily available, safe and inexpensive, and also protect against macrovascular complications of diabetes. Notably, ω -3PUFA-rich diets have the potential to prevent visual decline in the very early stages of DR before the clinical manifestation of the disease.

CONFLICT OF INTEREST

The authors declare no conflict of interest.

ACKNOWLEDGEMENTS

This work was supported by grants from the National Institutes of Health (EY017017, EY017017-04S1 (LEHS), EY020308 (JDA)), Children's Hospital Boston Mental Retardation and Developmental Disabilities Research Center (P01 HD18655 (LEHS)), Research to Prevent Blindness Senior Investigator Award (LEHS), Alcon Research Institute Award (LEHS), MacTel Foundation (LEHS), V Kann Rasmussen Foundation (LEHS), The Pearle Vision Foundation (JDA) and the William Randolph Hearst Fund (JDA). PS holds a Canada Research Chair in Retinal Cell Biology and is supported by grants from the Canadian Institutes of Health Research (CIHR; 221478), the CIHR Institute of Nutrition, Metabolism and Diabetes, The Canadian Diabetes Association (OG-3-11-3329-PS) and the Foundation Fighting Blindness Canada. Additional support was provided by the Juvenile Diabetes Research Foundation International, Children's Hospital Boston, the Manton Center for Orphan Disease Research and Charles H Hood Foundation (JC). AS is funded by Deutsche Forschungsgemeinschaft. Enzyme-linked immunosorbent assay experiments were performed with 5P30 DK 36836 Specialized Assay Core.

REFERENCES

- Kempner JH, O'Colmain BJ, Leske MC, Haffner SM, Klein R, Moss SE et al. The prevalence of diabetic retinopathy among adults in the United States. *Arch Ophthalmol* 2004; **122**: 552–563.
- Wild S, Roglic G, Green A, Sicree R, King H. Global prevalence of diabetes: estimates for the year 2000 and projections for 2030. *Diabetes Care* 2004; **27**: 1047–1053.
- Klein R, Klein BE, Moss SE, Davis MD, DeMets DL. The Wisconsin epidemiologic study of diabetic retinopathy. III. Prevalence and risk of diabetic retinopathy when age at diagnosis is 30 or more years. *Arch Ophthalmol* 1984; **102**: 527–532.
- Engerman RL, Kern TS. Retinopathy in animal models of diabetes. *Diabetes Metab Rev* 1995; **11**: 109–120.
- Barber AJ, Antonetti DA, Kern TS, Reiter CE, Soans RS, Krady JK et al. The Ins2Akita mouse as a model of early retinal complications in diabetes. *Invest Ophthalmol Vis Sci* 2005; **46**: 2210–2218.
- Barber AJ, Lieth E, Khin SA, Antonetti DA, Buchanan AG, Gardner TW. Neural apoptosis in the retina during experimental and human diabetes. Early onset and effect of insulin. *J Clin Invest* 1998; **102**: 783–791.
- Gastinger MJ, Kunselman AR, Conboy EE, Bronson SK, Barber AJ. Dendrite remodeling and other abnormalities in the retinal ganglion cells of Ins2 Akita diabetic mice. *Invest Ophthalmol Vis Sci* 2008; **49**: 2635–2642.
- Sapieha P, Hamel D, Shao Z, Rivera JC, Zaniolo K, Joyal JS et al. Proliferative retinopathies: angiogenesis that blinds. *Int J Biochem Cell Biol* 2010; **42**: 5–12.
- Chew EY, Ambrosius WT, Davis MD, Danis RP, Gangaputra S, Greven CM et al. Effects of medical therapies on retinopathy progression in type 2 diabetes. *N Engl J Med* 2010; **363**: 233–244.
- Lyons TJ, Jenkins AJ, Zheng D, Lackland DT, McGee D et al. Diabetic retinopathy and serum lipoprotein subclasses in the DCCT/EDIC cohort. *Invest Ophthalmol Vis Sci* 2004; **45**: 910–918.
- Keech AC, Mitchell P, Summanen PA, O'Day J, Davis TM, Moffitt MS et al. Effect of fenofibrate on the need for laser treatment for diabetic retinopathy (FIELD study): a randomised controlled trial. *Lancet* 2007; **370**: 1687–1697.
- SanGiovanni JP, Chew EY. The role of omega-3 long-chain polyunsaturated fatty acids in health and disease of the retina. *Prog Retin Eye Res* 2005; **24**: 87–138.
- Fetterman Jr JW, Zdanowicz MM. Therapeutic potential of n-3 polyunsaturated fatty acids in disease. *Am J Health Syst Pharm* 2009; **66**: 1169–1179.
- Connor KM, SanGiovanni JP, Lofqvist C, Aderman CM, Chen J, Higuchi A et al. Increased dietary intake of omega-3-polyunsaturated fatty acids reduces pathological retinal angiogenesis. *Nat Med* 2007; **13**: 868–873.
- Sapieha P, Stahl A, Chen J, Seaward MR, Willett KL, Krah NM et al. 5-Lipoxygenase metabolite 4-HDHA is a mediator of the antiangiogenic effect of (omega)-3 polyunsaturated fatty acids. *Sci Transl Med* 2011; **3**: 69ra12.
- Stahl A, Sapieha P, Connor KM, SanGiovanni JP, Chen J, Aderman CM et al. Short communication: PPAR gamma mediates a direct antiangiogenic effect of omega 3-PUFAs in proliferative retinopathy. *Circ Res* 2010; **107**: 495–500.
- SanGiovanni JP, Chew EY, Clemons TE, Davis MD, Ferris 3rd FL, Gensler GR et al. The relationship of dietary lipid intake and age-related macular degeneration in a case-control study: AREDS Report No. 20. *Arch Ophthalmol* 2007; **125**: 671–679.
- Abbatecola AM, Evans W, Paolisso G. PUFA supplements and type 2 diabetes in the elderly. *Curr Pharm Des* 2009; **15**: 4126–4134.
- Akula JD, Mocko JA, Benador IY, Hansen RM, Favazza TL, Vyhovsky TC et al. The neurovascular relation in oxygen-induced retinopathy. *Mol Vis* 2008; **14**: 2499–2508.
- Hood DC, Birch DG. A computational model of the amplitude and implicit time of the b-wave of the human ERG. *Vis Neurosci* 1992; **8**: 107–126.
- Lamb TD, Pugh Jr EN. A quantitative account of the activation steps involved in phototransduction in amphibian photoreceptors. *J Physiol* 1992; **449**: 719–758.
- Wurzig K, Lichtenberger T, Hanitzsch R. On-bipolar cells and depolarising third-order neurons as the origin of the ERG-b-wave in the RCS rat. *Vision Res* 2001; **41**: 1091–1101.
- Robson JG, Frishman LJ. Response linearity and kinetics of the cat retina: the bipolar cell component of the dark-adapted electroretinogram. *Vis Neurosci* 1995; **12**: 837–850.
- Akula JD, Lyubarsky AL, Naarendorp F. The sensitivity and spectral identity of the cones driving the b-wave of the rat electroretinogram. *Vis Neurosci* 2003; **20**: 109–117.
- Akula JD, Mocko JA, Moskowitz A, Hansen RM, Fulton AB. The oscillatory potentials of the dark-adapted electroretinogram in retinopathy of prematurity. *Invest Ophthalmol Vis Sci* 2007; **48**: 5788–5797.
- Kern TS, Engerman RL. A mouse model of diabetic retinopathy. *Arch Ophthalmol* 1996; **114**: 986–990.
- Kowluru RA, Engerman RL, Kern TS. Diabetes-induced metabolic abnormalities in myocardium: effect of antioxidant therapy. *Free Radic Res* 2000; **32**: 67–74.
- Zheng L, Du Y, Miller C, Gubitosi-Klug RA, Ball S, Berkowitz BA et al. Critical role of inducible nitric oxide synthase in degeneration of retinal capillaries in mice with streptozotocin-induced diabetes. *Diabetologia* 2007; **50**: 1987–1996.
- Shirao Y, Kawasaki K. Electrical responses from diabetic retina. *Prog Retin Eye Res* 1998; **17**: 59–76.
- Li Q, Zemel E, Miller B, Perlman I. Early retinal damage in experimental diabetes: electrophysiological and morphological observations. *Exp Eye Res* 2002; **74**: 615–625.
- Hancock HA, Kraft TW. Oscillatory potential analysis and ERGs of normal and diabetic rats. *Invest Ophthalmol Vis Sci* 2004; **45**: 1002–1008.
- Qin Q, Patel KA, Gronert K, Sharma SC. Neuroprotectin D1 inhibits retinal ganglion cell death following axotomy. *Prostaglandins Leukot Essent Fatty Acids* 2008; **79**: 201–207.
- Neschen S, Morino K, Dong J, Wang-Fischer Y, Cline GW, Romanelli AJ et al. n-3 Fatty acids preserve insulin sensitivity in vivo in a peroxisome proliferator-activated receptor-alpha-dependent manner. *Diabetes* 2007; **56**: 1034–1041.
- Storlien LH, Kraegen EW, Chisholm DJ, Ford GL, Bruce DG, Pascoe WS. Fish oil prevents insulin resistance induced by high-fat feeding in rats. *Science* 1987; **237**: 885–888.
- Oshitari T, Hanawa K, Adachi-Usami E. Changes of macular and RNFL thicknesses measured by Stratus OCT in patients with early stage diabetes. *Eye (Lond)* 2009; **23**: 884–889.
- Adamis AP, Berman AJ. Immunological mechanisms in the pathogenesis of diabetic retinopathy. *Semin Immunopathol* 2008; **30**: 65–84.
- Kowluru RA, Koppolu P. Diabetes-induced activation of caspase-3 in retina: effect of antioxidant therapy. *Free Radic Res* 2002; **36**: 993–999.
- Mohr S, Xi X, Tang J, Kern TS. Caspase activation in retinas of diabetic and galactosemic mice and diabetic patients. *Diabetes* 2002; **51**: 1172–1179.
- Dorrell MI, Aguilar E, Jacobson R, Yanes O, Gariano R, Heckenlively J et al. Anti-oxidant or neurotrophic factor treatment preserves function in a mouse model of neovascularization-associated oxidative stress. *J Clin Invest* 2009; **119**: 611–623.

- 40 Stahl A, Krohne TU, Sapieha P, Chen J, Hellstrom A, Chew E *et al*. Lipid metabolites in the pathogenesis and treatment of neovascular eye disease. *Br J Ophthalmol* 2011; **95**: 1496–1501.
- 41 Shue EH, Carson-Walter EB, Liu Y, Winans BN, Ali ZS, Chen J *et al*. Plasmalemmal vesicle associated protein-1 (PV-1) is a marker of blood-brain barrier disruption in rodent models. *BMC Neurosci* 2008; **9**: 29.
- 42 Keuschnigg J, Henttinen T, Auvinen K, Karikoski M, Salmi M, Jalkanen S. The prototype endothelial marker PAL-E is a leukocyte trafficking molecule. *Blood* 2009; **114**: 478–484.
- 43 Bensinger SJ, Tontonoz P. Integration of metabolism and inflammation by lipid-activated nuclear receptors. *Nature* 2008; **454**: 470–477.
- 44 Fehm HL, Kern W, Peters A. The selfish brain: competition for energy resources. *Prog Brain Res* 2006; **153**: 129–140.
- 45 Pardridge WM. Transport of insulin-related peptides and glucose across the blood-brain barrier. *Ann NY Acad Sci* 1993; **692**: 126–137.
- 46 Tomlinson DR, Gardiner NJ. Glucose neurotoxicity. *Nat Rev Neurosci* 2008; **9**: 36–45.



This work is licensed under the Creative Commons Attribution-NonCommercial-No Derivative Works 3.0 Unported License. To view a copy of this license, visit <http://creativecommons.org/licenses/by-nc-nd/3.0/>

Supplementary Information accompanies the paper on the Nutrition and Diabetes website (<http://www.nature.com/nutd>)